Proceedings of 10th IEEE International Conference
on Nanotechnology Joint Symposium with Nano Korea 2010
August 17~20, KINTEX, Korea

Spheres on Pillars: Nanobubbling Based on Attogram Mass Delivery from Metal-Filled Nanotubes

Zheng Fan[1], Xinyong Tao[2], Xudong Cui[3], Xudong Fan[4], and Lixin Dong[1,*]

[1]Department of Electrical and Computer Engineering, Michigan State University, East Lansing, MI 48824-1226, USA
[2]College of Chemical Engineering and Materials Science, Zhejiang University of Technology, Hangzhou 310014, China
[3]Department of Material Science & Technology, Research Center of Laser Fusion, China Academy of Engineering Physics, Mianyang, Sichuan 621900, China
[4]Center of Advance Microscopy, Michigan State University, East Lansing, MI 48824-1226, USA
*Email: ldong@egr.msu.edu

Abstract- ***We report an experimental investigation into the controlled fabrication of metallic nanospheres on the tip of nanotubes. The fabrication process, nanobubbling, is based on nanofluidic mass delivery at the attogram scale using metal-filled carbon nanotubes (CNTs). Two methods have been investigated including electron-beam-induced bubbling (EBIB) and electromigration-based bubbling (EMBB). Under the irradiation of a high energy electron beam of a transmission electron microscope (TEM), the encapsulated metal is melted and extruded out from the tip of the nanotube; generating a metallic sphere. Our investigation showed that several factors including temperatures, nanotube tip breaking/opening, and electron-beam-induced reconstruction of the carbon shells are responsible to the sizes and shapes of the metallic spheres on the nanotubes. In the case that the encapsulated materials inside the CNT has a higher melting point than that of the beam energy can reach, electromigration-based mass delivery is an optional process to apply. Results show that under a low bias (2-2.5V), spherical nanoparticles can be formed on the tips of nanotubes. EMBB is a further development of the nanorobotic spot welding technique and a fundamental technology for thermal dip pen nanolithography. The sphere-on-pillar structures and the nanobubbling processes proposed will enable devices such as nanooptical antennas, scanning near-field optical microscope (SNOM) probes, scanning anodes for field emitters, and single molecule detectors, which can find applications in bio-sensing, molecular detection, and high-resolution optical microscopy.***

I. Introduction

Nanospheres on pillars (tubes or wires) are of interest for potential fundamental and practical implications in areas such as nanophotonics, vacuum nanoelectronics, and bionanotechnology as optical antennas, apertureless scanning near-field optical microscopy (SNOM), scanning anodes for field emitters, and single molecule detectors [1-4]. A verity of techniques, such as inversed self-assembly grafting [5], wet-chemistry surface assembly [6], water-flow suction [7], photocatalytic deposition [8], and optical trapping [9], have been developed to attach metallic nanoparticles on a cantilever tip or an optical fiber, however, the controlled attachment of individual nanoparticles on nanopillars has been shown infeasible [10].

Carbon nanotubes (CNTs) are ideal building blocks for the pillars because of their well-defined structures and remarkable mechanical/electronic properties. Furthermore, the hollow cavities of CNTs allow varieties of materials to be encapsulated such as metals [11], fullerenes [12] and water [13], which are primary candidates for the study of nanofluidic system. Previous investigations have focused on delivering the encapsulated materials intra-/inter-carbon shells [14-17]. In the previous investigation of single crystalline copper encapsulated nanotubes for nanorobotic spot welding, we found that we were able to induce in a controlled way the melting and flowing of the single crystalline copper from individual CNTs [14, 17] using a very low bias, which is due to the very low binding energy of Cu to the CNTs (0.1-0.144 eV). By delivering the encapsulated materials from the carbon shells, here we present that nanospheres can be bubbled over the CNT tips. This is a novel process with potential for the fabrication of spherical nanostructures, whereas other additive lithography processes such as electron-beam-induced deposition (EBID) [18], focused-ion-beam chemical vapor deposition (FIB-CVD) [19], or lasers [20] are hardly attainable.

Many metals and their alloys such as Cu, Sn, Zn, Ni, Fe, and Co can be encapsulated into CNTs, which are ideal building blocks for the generation of nanospheres on CNT tips. The fabrication processes, named nanobubbling, resemble blowing a balloon using a pipe, and technically it is based on nanofluidic mass delivery at the attogram scale [21] by using metal-filled CNTs (m@CNTs). Two processes have been investigated, i.e., electron-beam-induced bubbling (EBIB) and electromigration-based bubbling (EMBB). In previous works, electron-beam-induced expansion, melting, and flowing of the encapsulated materials inside a nanotube have been observed, and potential applications such as thermometers and extruders have been demonstrated [22-24]. Previous investigations on the intra- and inter-nanotube mass melting, flowing, evaporation, and delivery based on electromigration have enabled new techniques such as nanorobotic spot welding [14] and devices such as archival memories [25]. Bubbling involves some novel aspects such as pressure accumulation inside nanotubes, nanotube tip breaking or opening, and shaping and sizing of the particles.

978-1-4244-7032-7/10/$26.00 ©2010 IEEE

II. Experimental Setup

Our experiments were performed in a transmission electron microscope (TEM, JEOL 2200FS) with a field emission gun. The samples we used include Sn- and Cu-filled CNTs. The Sn@CNTs samples were synthesized by using catalytic deposition of acetylene using SnO_2 [24]. During the process, the catalysts were directly into the furnace and without the preheating and reduction process. The Sn@CNTs have diameters distributed from 20 to 80 nm. Sn cores are single crystal with good crystallization. The Cu-tipped CNTs are synthesized using an alkali-doped Cu catalyst by a thermal CVD method, and their outer diameters are in a range of 40-80 nm. The single crystalline Cu nanoneedles are encapsulated in graphite walls approximately 4 to 6 nm thick at the tips of CNTs. Figure 1 (a) to (d) show the TEM images of their structures.

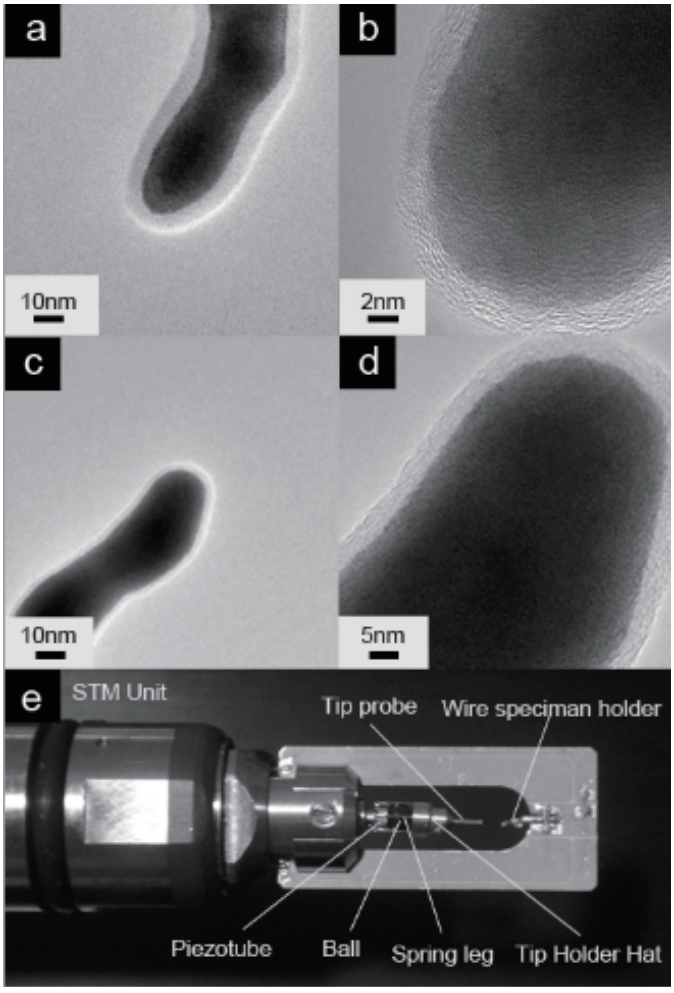

Figure 1. (a-b) Sn-filled CNTs. (a) TEM images of Sn-filled CNTs. The image shows that the CNT is filled with metal nanowires. These carbon nanotubes are with the outer diameters in a range of 20-80nm; (b) TEM images of Sn@CNTs synthesized at 610 °C for 30 min, the locally magnified HRTEM of the tip region of the CNT in (a). (c) TEM image of Cu-filled CNTs. (d) The locally magnified HRTEM image of the rectangular tip region of the CNT in (c). (e) FM2000E STM-TEM holder (Nanofactory Instruments AB).

A single-tilt TEM holder is used for EBIB and a scanning tunneling microscope built in a TEM holder (Nanofactory Instruments AB) is adopted for EMBB. Figure 1 (e) is the structure of the FM2000E STM-TEM holder.

III. EBIB of Sn-filled CNTs

During the EBIB, the current density of the electron beam transmitting through the CNTs was adjusted by changing the beam convergence as well as the magnification and the incident area. The final shapes can be either spheres or particles with facets, which are related to the heating and cooling processes. The sizes of the spheres on the tips are found to be related to the exposure time and the orifices of the nanotube. Figure 2 (a) to (j) show the EBIB (as schematically shown in Fig. 2 (k)) of Sn@CNT at a current density of 20 A/cm^2 with the magnification of ×300K and the irradiation area of 1.3×10^{-14} cm^2 increasing the current density, the local temperature would increase due to the increase of the electron energy. The process was recorded by TEM images. Starting from an as-synthesized Sn-filled CNT, it can be seen that a nanosphere has been formed on the tip of the CNT due to the exposure to the electron beam. At t = 720 s (Fig. 2(d)), the inner molten metal first broke out of the nanotube. In our previous investigations, we have observed that the tin nanowire would melt entirely in the CNTs when the current density reaches 0.4 A/cm^2, and the expansion of the tin wire would occur at the same time [24] (Fig. 2(b)), but this is the first time we observe the bubbling of the molten metal. At the beginning of the process, polyhedral nanoparticles (Fig. 2(g) and (h)) will be formed. By increasing temperatures, it is possible to convert polyhedral nanoparticles into spheres (Fig. 2(j)) [26]. We attribute the bubbling and the shape conversion to the electron irradiation and the secondary effects including the carbon shell contraction and the surface tension of the molten metal. The encapsulated materials were melted and then squeezed out by the carbon shells as spheres onto the top of nanotubes. Applying an image processing method, the mass of the sphere is analyzed. The CNT has an external diameter of approximately 40nm. The diameter of the final sphere is 54 nm, and the mass of the resulted sphere is 0.6 fg (femtograms) according to the density of the tin (7.31 g/cm^3). A curve of the time for the bubbling vs. the diameter of the sphere is depicted in Fig. 2 (l).

It is found that the threshold current density for the sphere formation is 20 A/cm^2 with the exposure time of ~720 s. Experiments on several CNTs showed that the threshold current density varies from 10 to 25 A/cm^2 due to the diameters of the CNTs (37-40 nm). The current density is adjusted by changing the focus (beam diameter and brightness) of the electron beam and the magnifications. The accelerating voltage is 200 kV.

According to the experiments, the EBIB process consists of two parts, i.e., the melting of the inner metal and the shrinkage of the carbon shells. The melting was due to the heating of the tin by the irradiation effects as revealed in previous works [24].

As a result, thermal expansion [22, 27] will cause the accumulation of internal pressure inside carbon shells. In previous experiments [24], the authors reported that the melting occurred with equal probability under different accelerating voltages, which means that atomic displacements are not the main reason that the nanowire melts, rather the temperature rise caused by the electron beam irradiation results in the melting of the nanowire.

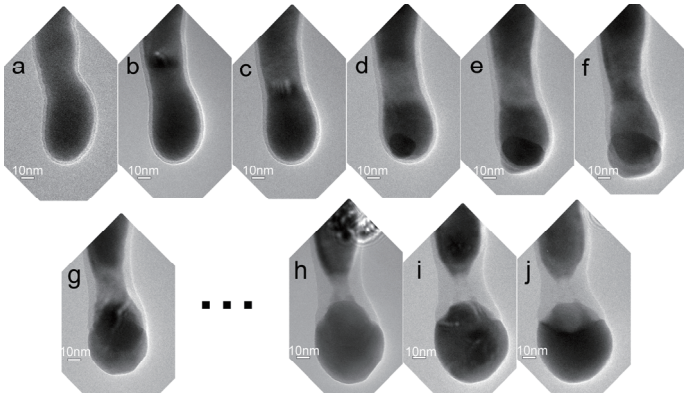

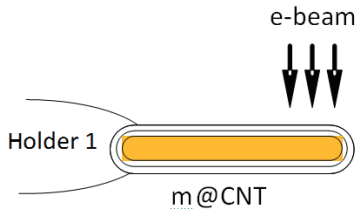

(k)

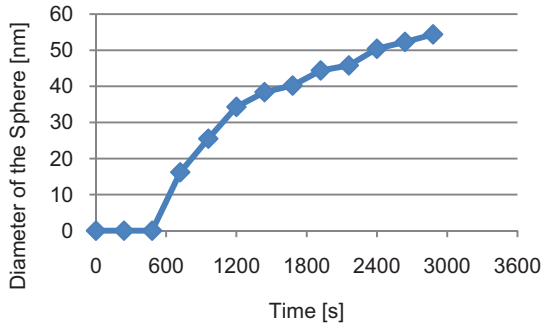

(l)

Figure 2. TEM images of Sn@CNT bubbling. (a) A Sn-filled CNT was brought to under the exposure of electron beam at t=0. (b, c) Under the current density of 20A/cm^2 from 240s to 480s, a molten section of tin appeared and moved to the tip of the tube and the tube become more spherical because of the melting occurred. (d) At t=720s, the inner metal was first break out of the tube. (e, f) On the effects of the electron irradiation, the flow out of metal continues, and the carbon shell near the tip of tube largely deform which may be responsible to the squeezing out of the sphere from the nanotube shell. (g) At t=1440s, a sphere is visible on the tip of CNT; (h)(i) The sphere shape was completed at t=2400s. (i, j) At t=2880s, the sphere on the tip completed, the shrinkage of the carbon shell prevented the metal flow from the bottom to the top of the tube. (k) The schematic of EBIB. (l) shows the configuration of the characterization of the diameter of the sphere vs. the time at the current density of 20 A/cm^2.

Previous experimental observations of the radiation damage in graphite by high-resolution electron microscopy at room temperature have shown the defect formation on carbon layers [28]. As a result, the defects on the carbon shell will allow the bubbling occurs. This can be explained by the rupture of planes and the formation of dislocation loops during the agglomeration of interstitials (Fig. 3 (a)). Agglomerates form when two displaced atoms diffuse two dimensionally between two basal planes and combine to form a less mobile group. Other displaced atoms condense on to this nucleus which then grows into a disc, pushing the adjacent basal planes apart. Continued aggregation leads to the formation of a new lattice plane. However, due to the existing of the encapsulated materials, the rapture of the carbon plane may not purely caused by the decomposing of the carbon shells, the internal pressure also contributed to the bubbling (Fig. 3 (b)).

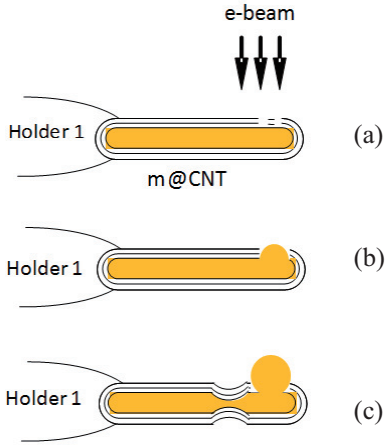

Figure 3. The decompose of carbon shell. (a) Displacement of atom caused the rupture of planes; (b) Flow out of the inner metal; (c) The self contraction caused continuing flow out of molten metal prevent the self-reconstruction of carbon shell.

The displacement energy E_d is the kinetic energy required to displace an atom from its original lattice position to an unstable one. The displacement cross section σ_d, which represents the probability that an electron with energy E_p can displace an atom as the area of a target, is given by [28, 29]

$$\sigma_d = Z^2 4\pi a_0^2 U_R^2 \left(\frac{1-\beta^2}{m^2c^4\beta^4}\right)\left[\frac{E_{max}}{E_d} + 2\pi\alpha\beta\sqrt{\frac{E_{max}}{E_d}} - (\beta^2 + \pi\alpha\beta) \times \ln\left(\frac{E_{max}}{E_d}\right) - (1 + 2\pi\alpha\beta)\right] \quad (1)$$

where $E_{max} = 2E_p(E_p + 2mc^2)/Mc^2$, M is the mass of the nucleus, a_0 is the Bohr radius $(5.29 \times 10^{-11}\ m)$, U_R is the Rydberg energy (13.6 eV), Z is the atomic number of the nucleus, and α = Z/137. The incident electron energy E_p is determined by the equation $E_p = mc^2[(1-\beta^2)^{1/2} - 1]$, where m is the rest mass of the electron, c is the speed of light, υ is the velocity of the electron, and $\beta = \upsilon/c$. The threshold displacement energy of carbon is 25 eV [30], and the displacement cross section σ_d for the carbon is largely decreased when the incident electron energy decreased at 200

keV (Fig. 4), which is the working energy in our experiment, therefore the displacement cross section in this incident energy is very low and may not be responsible for the bubbling.

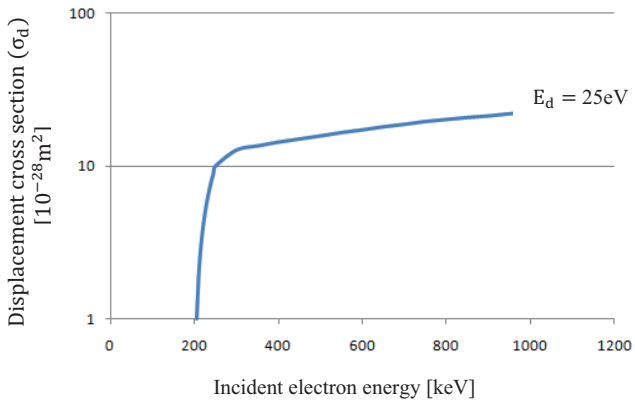

Figure 4. Displacement cross section with different incident electron energy for the carbon (E_d = 25eV).

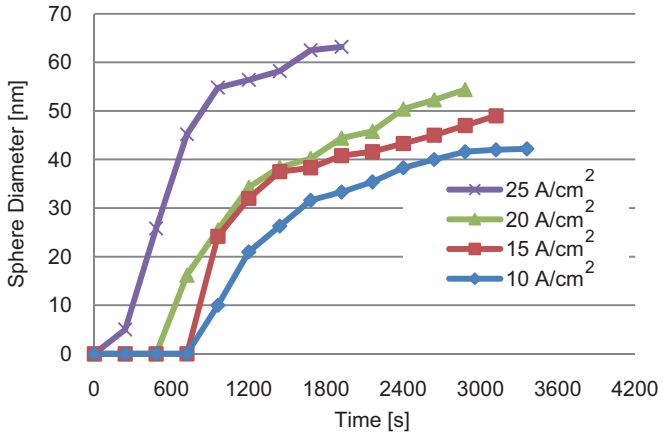

Figure 5. Time sequence of bubbling at different current densities.

Hence, the rapture of the carbon plane caused by irradiation effects is the reason for the decomposition of the carbon shell. Furthermore, the contraction of the carbon shells being observed (Fig. 2 (d)-(g)), is responsible for the squeezing out of the sphere from the nanotube shell, that is because controlled electron beam irradiation on CNTs may cause large pressure within the nanotube cores that can deform and extrude the metals from the carbon shells [23]. In a similar carbon onion structure, such pressure can be enormous to cause the inner shells converting into a nano-diamond [31]. So, the full process is like this: the rapture of the carbon plane makes the defects on the carbon shell, then the bubbling occurred at the defects (Fig. 3 (b) and (c)). The internal pressure accumulation is a result of the melting and thermal expansion of the encapsulated metal, and the shrinkage of the nanotube shells [23], which are all determined by the current density. As a result, the rates of the nanobubbling and the geometry of the spheres can be controlled by the adjusting of the current density.

The dependence has been invetigated with several Sn@CNT (diameters: 37-40 nm) at the irradiation current density varying from 10~25A/cm^2. Figure 5 shows the time sequence of the diameter changes of the nanospheres. It can be found that, with the increase of irradiation energy, the starting time for the flowing out is shortened. The starting time varies from 200 s-700 s for the current density from 10~25 A/cm^2, and the bubbling time varies from 1900s~3360s.

IV. EMBB of Cu-filled CNTs

The same EBIB procedures have been applied to Cu-filled CNTs, but bubbling did not start at the highest possible current density. That implies that the e-beam from the TEM cannot reach the melting point of copper. As an alternative method, EMBB has been developed for Cu-filled CNTs. A scanning tunneling microscope built in a TEM holder, FM2000E STM-TEM holder (Nanofactory Instruments AB), is adopted for EMBB (Fig. 1 (e)). The probe can be positioned in a millimeter-scale workspace with subnanometer resolution with the STM unit actuated by a three-degree-of-freedom piezotube, making it possible to select a specific CNT. Physical contact can be made between the probe and the tip of a nanotube. Applying a voltage between the probe and the sample holder establishes an electrical circuit through a CNT and injects thermal energy into the system via Joule heating. By increasing the applied voltage, the local temperature can be increased past the melting point of the copper encapsulated in a tube. Then, the encapsulated materials may deliver from the carbon shells, and nanospheres are bubbled over the CNT tips. The EMBB process is similar to nanorobotic spot welding [14], but the focus is on the shape and size control of the deposited spots. During the experiments, the intensity of the electron beam has been kept in the range for regular imaging, which is several order of magnitude lower that the above-mentioned values.

In the experiments, the Cu-filled CNT tip was first brought to contact with the STM probe, and then apply a bias voltage on the two ends of the CNT. With the increasing of the voltage from 0 V on the step of 0.1 V, when it reached the range between 2.0 V to 2.5 V, the inner copper core flowed out to the tip of CNT in a short time. The process was recorded by real-time video, and the selected video frames of the melting process (Fig. 6 (a)) reveal that, a copper polyhedral nanoparticle formed initially on the tip of the tube (Fig. 6 (b)). Then, by increasing the bias (the temperature), a spherical particles can be formed on the tip of nanotubes (Fig. 6 (c)). In this experiment, the flow out of the copper was started at 2.4 V, the entire process continued for about 17 s, and the flow rate was found to be about 82.3 nm/s according to the length change of the inner copper core (Fig. 6(a)). The current vs. voltage curves were obtained before and after the copper flowed out (Fig. 6 (e)). Comparing the two I-V curves, we found that the current through the CNT before flowing was larger than the current after the flowing occurred. That is a result of the exposure of the carbon shells due to the loss of the

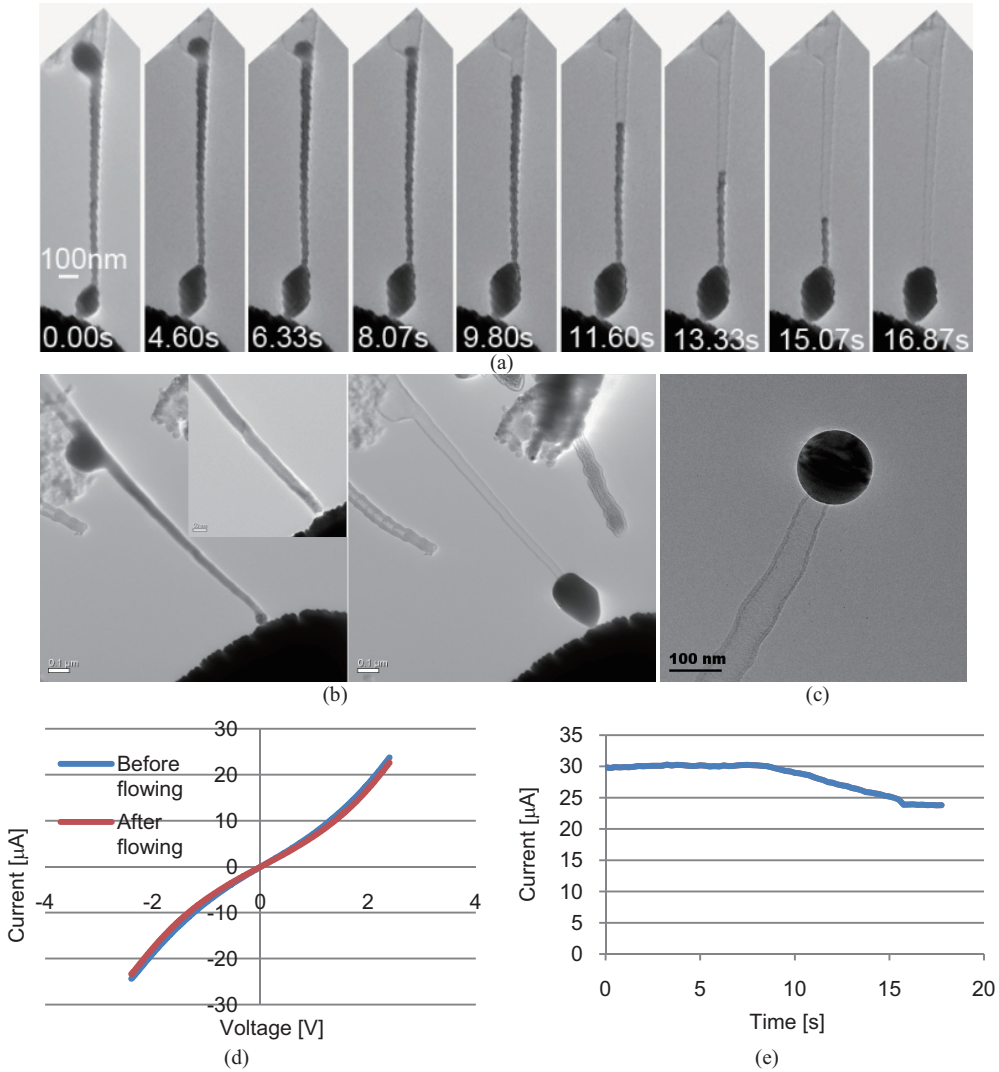

Figure 6. EMBB processes. (a) EMBB using a copper-filled CNT. (b) Sphere on the tip by EMBB. (c) A sphere formed on a nanotube. (d) I-V characterization. (e) I-t characterization.

encapsulated copper, which has better conductivity than carbon. The real-time current-time curve recorded by a multimeter (Fig. 6(f)) during the copper flowing out also showed that the current decreased along with the flowing time.

Accordingly, the current density under the bias of 2.4 V dropped from 2.38×10^6 A/cm^2 to 1.98×10^6 A/cm^2, causing the cooling down of the deposit at the orifice. Moreover, heat dissipation increased when more copper reached to the probe. As the volume of the probe (tip radius: 70 nm, root radius: 10 μm) is absolutely larger than that of the copper deposit, the probe serves as a heat sink with essentially infinite capacity comparing with the copper deposit. Hence, reheating up the copper would not be possible after cooling down. This can explain why the flowed out materials crystallized immediately while the bias kept unchanged, and in most cases, without increasing the bias during the flowing, polyhedral nanoparticles will be formed.

The melting of the copper core was due to the Joule heating of the copper by the current passing through the carbon shells. The highest temperature appears at the middle point of the tube. Theoretically, by controlling the mass flowing out, we can control the size of nanospheres. However, the heat capacitance of the target significantly influences the process. To generate a sphere on the tip of a CNT, in practice, we can compensate the dropped current with a higher bias or use another CNT as the target. While it is yet well understood quantitatively, the heat transport changed due to the draining of the CNT must be taken into consideration when designing the process for EMBB, spot welding, and thermal dip pen nanolithography [14] using metal-filled CNTs.

V. Conclusions

In summary, we have proposed EBIB and EMBB for the fabrications of nanospheres on nanopillars. Controlled melting and bubbling of tin inside nanotube shells have been realized at the current density of 10~25 A/cm^2. Bubbling started after the Sn@CNTs having been exposed under the electron beam for 1900 s to 3360 s based on their sizes. The melting of the encapsulated tin is the result of the carbon displacement threshold energy reached by the beam irradiation, which is also

the reason of the destruction of carbon shell. The beam irradiation caused internal pressure accumulation that is attributed to the melting and thermal expansion of the encapsulated materials and the shrinkage of the nanotube shells, which finally pushed out the molten metal and formed bubbles. EBIB does not need to make a contact of the nanotube to an electrode; hence featured with simplicity. However, the process is time-consuming and involves high energy beam. The highest achievable temperature is limited by the intensity of the electron beam. The best application can be found in encapsulated materials with a low melting point. To the materials with a high melting point, EMBB is a method to applied, by applying a bias voltage of as low as 2 - 2.5 V, the bubbling have been realized with Cu-filled CNTs. The copper-filled CNTs in the experiment has a 40-nm diameter, and the flowing has continued for 17 s at the flow rate of 82.3 nm/s and the bias threshold for the flowing is 2.4 V. Due to the contact between the CNT tip and an counter electrode, new challenges raised to the process. The heat sink into the electrodes may cause the immediate cooling and re-crystallization of the deposits during the draining of the CNT, which becomes a common challenge to the process design for EMBB, spot welding, and thermal dip pen nanolithography using metal-filled CNTs if specific shapes, continuous writing, and reshaping are expected. The sphere-on-pillar structures and nanobubbling process are expected to find applications in bio-sensing, molecular detection, and high-resolution optical microscopy.

REFERENCES

[1] L. Novotny, "Nano-optics - Optical antennas tuned to pitch," *Nature,* vol. 455, pp. 887-887, Oct 2008.

[2] P. Muhlschlegel, H. J. Eisler, O. J. F. Martin, B. Hecht, and D. W. Pohl, "Resonant optical antennas," *Science,* vol. 308, pp. 1607-1609, Jun 2005.

[3] P. Anger, P. Bharadwaj, and L. Novotny, "Enhancement and quenching of single-molecule fluorescence," *Physical Review Letters,* vol. 96, art. no. 113002, Mar 2006.

[4] T. Kalkbrenner, M. Ramstein, J. Mlynek, and V. Sandoghdar, "A single gold particle as a probe for apertureless scanning near-field optical microscopy," *Journal of Microscopy-Oxford,* vol. 202, pp. 72-76, Apr 2001.

[5] O. Sqalli, M. P. Bernal, P. Hoffmann, and F. Marquis-Weible, "Improved tip performance for scanning near-field optical microscopy by the attachment of a single gold nanoparticle," *Applied Physics Letters,* vol. 76, pp. 2134-2136, Apr 2000.

[6] I. U. Vakarelski and K. Higashitani, "Single-nanoparticle-terminated tips for scanning probe microscopy," *Langmuir,* vol. 22, pp. 2931-2934, Mar 2006.

[7] Y. Kawata, S. Urahama, M. Murakami, and F. Iwata, "The use of capillary force for fabricating probe tips for scattering-type near-field scanning optical microscopes," *Applied Physics Letters,* vol. 82, pp. 1598-1600, Mar 2003.

[8] T. Okamoto and I. Yamaguchi, "Photocatalytic deposition of a gold nanoparticle onto the top of a SiN cantilever tip," *Journal of Microscopy-Oxford,* vol. 202, pp. 100-103, Apr 2001.

[9] F. Pampaloni, G. Lattanzi, A. Jonas, T. Surrey, E. Frey, and E. L. Florin, "Thermal fluctuations of grafted microtubules provide evidence of a length-dependent persistence length," *Proceedings of the National Academy of Sciences of the United States of America,* vol. 103, pp. 10248-10253, Jul 2006.

[10] Y. Gan, "A review of techniques for attaching micro- and nanoparticles to a probe's tip for surface force and near-field optical measurements," *Review of Scientific Instruments,* vol. 78, art. no. 081101, Aug 2007.

[11] X. Y. Tao, X. B. Zhang, J. P. Cheng, Z. Q. Luo, S. M. Zhou, and F. Liu, "Thermal CVD synthesis of carbon nanotubes filled with single-crystalline Cu nanoneedles at tips," *Diamond and Related Materials,* vol. 15, pp. 1271-1275, Sep 2006.

[12] B. W. Smith, M. Monthioux, and D. E. Luzzi, "Encapsulated C-60 in carbon nanotubes," *Nature,* vol. 396, pp. 323-324, Nov 1998.

[13] Y. Gogotsi, J. A. Libera, A. Guvenc-Yazicioglu, and C. M. Megaridis, "In situ multiphase fluid experiments in hydrothermal carbon nanotubes," *Applied Physics Letters,* vol. 79, pp. 1021-1023, Aug 2001.

[14] L. X. Dong, X. Y. Tao, L. Zhang, X. B. Zhang, and B. J. Nelson, "Nanorobotic spot welding: Controlled metal deposition with attogram precision from copper-filled carbon nanotubes," *Nano Letters,* vol. 7, pp. 58-63, art. no. 10.1021/nl061980+, 2007.

[15] L. X. Dong, X. Y. Tao, M. Hamdi, L. Zhang, X. B. Zhang, A. Ferreira, and B. J. Nelson, "Nanotube fluidic junctions: Inter-nanotube attogram mass transport through walls," *Nano Letters,* vol. 9, pp. 210-214, Jan 2009.

[16] L. X. Dong, X. Y. Tao, M. Hamdi, L. Zhang, X. B. Zhang, A. Ferreira, and B. J. Nelson, "Nanotube boiler: Attogram copper evaporation driven by electric current, Joule heating, charge, and ionization," *IEEE Transactions on Nanotechnology,* vol. 8, pp. 565-568, Sep 2009.

[17] D. Golberg, P. Costa, M. Mitome, S. Hampel, D. Haase, C. Mueller, A. Leonhardt, and Y. Bando, "Copper-filled carbon nanotubes: Rheostatlike Behavior and femtogram copper mass transport," *Advanced Materials,* vol. 19, pp. 1937-1942, Aug 2007.

[18] L. X. Dong, F. Arai, and T. Fukuda, "Electron-beam-induced deposition with carbon nanotube emitters," *Applied Physics Letters,* vol. 81, pp. 1919-1921, Sept. 2002.

[19] R. Kometani, K. Kanda, Y. Haruyama, T. Kaito, and S. Matsui, "Evaluation of field electron emitter fabricated using focused-ion-beam chemical vapor deposition," *Japanese Journal of Applied Physics Part 2-Letters & Express Letters,* vol. 45, pp. L711-L713, Jul 2006.

[20] P. Kral and D. Tomanek, "Laser-driven atomic pump," *Physical Review Letters,* vol. 82, pp. 5373-5376, Jun 1999.

[21] L. X. Dong, X. Y. Tao, L. Zhang, X. B. Zhang, and B. J. Nelson, "Plumbing the depths of the nanometer scale: Attogram mass transport via nanochannels," *IEEE Nanotechnology Magazine,* vol. 4, pp. 13-22, Mar 2010.

[22] Y. H. Gao and Y. Bando, "Carbon nanothermometer containing gallium - Gallium's macroscopic properties are retained on a miniature scale in this nanodevice," *Nature,* vol. 415, p. 599, Feb 2002.

[23] L. Sun, F. Banhart, A. V. Krasheninnikov, J. A. Rodriguez-Manzo, M. Terrones, and P. M. Ajayan, "Carbon nanotubes as high-pressure cylinders and nanoextruders," *Science,* vol. 312, pp. 1199-1202, May 2006.

[24] X. Y. Tao, L. X. Dong, W. K. Zhang, X. B. Zhang, J. P. Cheng, H. Huang, and Y. P. Gan, "Controllable Melting and Flow of β-Sn in Flexible Amorphous Carbon Nanotubes," *Carbon,* vol. 47, pp. 3122-3127, Nov. 2009.

[25] G. E. Begtrup, W. Gannett, T. D. Yuzvinsky, V. H. Crespi, and A. Zettl, "Nanoscale reversible mass transport for archival memory," *Nano Letters,* vol. 9, pp. 1835-1838, May 2009.

[26] X. D. Feng, D. C. Sayle, Z. L. Wang, M. S. Paras, B. Santora, A. C. Sutorik, T. X. T. Sayle, Y. Yang, Y. Ding, X. D. Wang, and Y. S. Her, "Converting ceria polyhedral nanoparticles into single-crystal nanospheres," *Science,* vol. 312, pp. 1504-1508, Jun 2006.

[27] D. Golberg, Y. B. Li, M. Mitome, and Y. Bando, "Real-time observation of liquid Indium unusual behavior inside silica nanotubes," *Chemical Physics Letters,* vol. 409, pp. 75-80, Jun 2005.

[28] F. Banhart, "Irradiation effects in carbon nanostructures," *Reports on Progress in Physics,* vol. 62, pp. 1181-1221, 1999.

[29] T. Yokota, M. Murayama, and J. M. Howe, "In situ transmission-electron-microscopy investigation of melting in submicron Al-Si alloy particles under electron-beam irradiation," *Physical Review Letters,* vol. 91, art. no. 265504, Dec 2003.

[30] T. Kamimura, K. Yamamoto, T. Kawai, and K. Matsumoto, "n-type doping for single-walled carbon nanotubes by oxygen ion implantation with 25 eV ultralow-energy ion beam," *Japanese Journal of Applied Physics Part 1-Regular Papers Brief Communications & Review Papers,* vol. 44, pp. 8237-8239, Nov 2005.

[31] F. Banhart and P. M. Ajayan, "Carbon onions as nanoscopic pressure cells for diamond formation," *Nature,* vol. 382, pp. 433-435, Aug 1996.